Published in final edited form as:

Mamm Genome. 2016 February ; 27(1-2): 29–46. doi:10.1007/s00335-015-9614-7.

The GPSM2/LGN GoLoco motifs are essential for hearing

Yoni Bhonker[1], **Amal Abu-Rayyan**[2], **Kathy Ushakov**[1], **Liat Amir-Zilberstein**[3], **Shaked Shivatzki**[1], **Ofer Yizhar-Barnea**[1], **Tal Elkan-Miller**[1], **Einav Tayeb-Fligelman**[5], **Sun Myoung Kim**[4], **Meytal Landau**[5], **Moien Kanaan**[2], **Ping Chen**[4], **Fumio Matsuzaki**[6], **David Sprinzak**[3], and **Karen B. Avraham**[1]

[1]Department of Human Molecular Genetics and Biochemistry, Sackler Faculty of Medicine and Sagol School of Neuroscience, Tel Aviv University, Tel Aviv 6997801, Israel

[2]Department of Biological Sciences, Bethlehem University, Bethlehem, Palestine

[3]Department of Biochemistry and Molecular Biology, Weiss Faculty of Life Sciences, Tel Aviv University, 69978 Tel Aviv, Israel

[4]Department of Cell Biology, Emory University, Atlanta, GA 30322, USA

[5]Department of Biology, Technion-Israel Institute of Technology, 32000 Haifa, Israel

[6]Laboratory of Cell Asymmetry, Center for Developmental Biology, Riken, Kobe 650-0047, Japan

Abstract

The planar cell polarity (PCP) pathway is responsible for polarizing and orienting cochlear hair cells during development through movement of a primary cilium, the kinocilium. GPSM2/LGN, a mitotic spindle-orienting protein associated with deafness in humans, is a PCP effector involved in kinocilium migration. Here, we link human and mouse truncating mutations in the *GPSM2*/*LGN* gene, both leading to hearing loss. The human variant, p.(Trp326*), was identified by targeted genomic enrichment of genes associated with deafness, followed by massively parallel sequencing. $Lgn^{\Delta C}$ mice, with a targeted deletion truncating the C-terminal GoLoco motifs, are profoundly deaf and show misorientation of the hair bundle and severe malformations in stereocilia shape that deteriorates over time. Full-length protein levels are greatly reduced in mutant mice, with upregulated mRNA levels. The truncated $Lgn^{\Delta C}$ allele is translated in vitro, suggesting that mutant mice may have partially functioning Lgn. Gαi and aPKC, known to function in the same pathway as Lgn, are dependent on Lgn for proper localization. The polarization of core PCP proteins is not affected in Lgn mutants; however, Lgn and Gαi are misoriented in a PCP mutant, supporting the role of Lgn as a PCP effector. The kinocilium, previously shown to be dependent on Lgn for robust localization, is essential for proper localization of Lgn, as well as Gαi and aPKC, suggesting that cilium function plays a role in positioning of apical proteins. Taken together, our data provide a mechanism for the loss of hearing found in human patients with *GPSM2*/*LGN* variants.

Correspondence to: Karen B. Avraham.

Compliance with ethical standards

Conflict of Interest The authors declare that they have no conflict of interest.

Electronic supplementary material The online version of this article (doi:10.1007/s00335-015-9614-7) contains supplementary material, which is available to authorized users.

Introduction

Almost 100 genes are known to be associated with human hearing loss, the most common sensory defect in humans (Shearer and Smith 2015). This genetic heterogeneity often makes genetic diagnosis difficult using conventional methods that address only one gene at a time. Developments in high-throughput sequencing have been a boon to the clinical diagnostics field (Gilissen et al. 2012) and in hearing impairment in particular (Brownstein et al. 2012; Shearer and Smith 2015). Identification of genes involved in hearing provides unique opportunities to gain a deeper understanding of inner ear function. Functional studies of the proteins these genes encode, carried out in mouse models for human deafness, have greatly expanded our understanding of how this complex organ is formed and how it converts mechanical stimuli into electrical signals (Bhonker et al. 2014; Richardson et al. 2011). This approach has uncovered novel genes whose involvement in inner ear development would likely not have been predicted based on its known role in other tissues. An example is Gpsm2, G-protein signaling modulator 2, a mitotic spindle-orienting protein (Mochizuki et al. 1996). Gpsm2 was not implicated as having a role in the inner ear until it was found to be associated with hearing loss (Walsh et al. 2010). Pathogenic variants in *GPSM2* were subsequently identified as the cause of a syndromic form of hearing loss, Chudley-McCullough syndrome (CMCS, OMIM #604213) (Walsh et al. 2010; Doherty et al. 2012). Localization of Gpsm2 in the mouse inner ear led to the hypothesis that this protein is involved in planar cell polarity (PCP) in the inner ear (Walsh et al. 2010).

Gpsm2, referred to as Lgn for its leucine-glycine-asparagine repeats, is a 684 amino acid protein highly conserved across eukaryotes. Hereafter, the mouse gene and protein will be referred to as Lgn. Identified as the mammalian homolog of the *Drosophila* Pins proteins (Du and Macara 2004), Lgn is an important player in asymmetric cell division in neuroblasts (Schaefer et al. 2000). Lgn contains four C-terminal GoLoco motifs that mediate its physical interaction with Gαi proteins (Tall and Gilman 2005). Gαi proteins are anchored to the cortical membrane via myristoyl groups, in cells in which they function in spindle orientation, and are necessary to localize Lgn to the apical cortex. Lgn's N-terminus contains seven tetratricopeptide (TPR) motifs, which interact with the nuclear protein NuMA during mitosis. Contact with NuMA partially opens Lgn, increasing its affinity for the cortically bound Gαi (Du and Macara 2004). These proteins form a conserved core ternary complex that is required to orient the mitotic spindle during cell division (for review see Stevermann and Liakopoulos 2012). Lgn binds Insc, responsible for coupling cell polarity and spindle orientation (Mauser and Prehoda 2012) by the former's N-terminus in a manner that excludes NuMA (Mapelli and Gonzalez 2012).

Spindle orientation is crucial for maintenance of all dividing cells within the plane of the tissue (Williams et al. 2011), as well as segregation of cell fate determinants in a symmetric or asymmetric fashion, thereby promoting self-renewal or differentiation of neuropepithelial progenitor cells (Konno et al. 2008). The central role of Lgn in cell division suggests that deleterious mutations would be lethal. A strong knockdown of Lgn in murine skin causes defects in barrier function, resulting in dehydration and death (Williams et al. 2011). In

contrast, all reported truncating human variants in GPSM2/LGN are viable (Walsh et al. 2010; Yariz et al. 2012; Doherty et al. 2012; Diaz-Horta et al. 2012; Almomani et al. 2013).

Cochlear hair cells become post-mitotic between embryonic days 13–14 (E13–E14; Wang et al. 2005), after which time they continue to differentiate and functionally mature. Cells in the organ of Corti then project a non-motile primary cilium, the kinocilium, at the center of their apical surface. This cilium, anchored to the cell via a centriolar basal body, migrates to the lateral edge of the apical surface and associates with the hair bundle, a structure comprised actin-based projections called stereocilia. The final orientation of the hair bundle is tightly correlated with the position of the kinocilium (Schwander et al. 2010). In the absence of a kinocilium, the orientation of the hair bundle becomes more random; however, hair bundle orientation still roughly correlates with the position of the basal body (Jones et al. 2007). Basal body migration has emerged as a key determinant of hair bundle morphogenesis.

Lgn and its pathway partners may act as a morphogen gradient to determine the shape of the mature hair bundle (Jacobo and Hudspeth 2014). Speculating that the same proteins that control mitotic spindle orientation also control kinocilium movement in hair cells, an inner ear conditional knock-out mouse of Lgn (termed *mPins* cKO) was examined and shown to have a more centrally positioned and less constrained kinocilia (Ezan et al. 2013). In a study designed to address the role of the bare zone, the apical region of hair cells that lacks microvilli, the interaction between Lgn and Gαi was examined in the Lgn mouse mutant Lgn^{BF}s with a truncation after the second TPR motif (Tarchini et al. 2013). Both proteins are polarized in this apical zone and along with aPKC and mInsc, were implicated in establishing the distribution of stereocilia and the kinocilium, and are thus a major determinant of hair cell planar cell polarity.

Here, we report the identification of a novel human *GPSM2* pathogenic variant by Targeted Gene Enrichment (TGE) and Massively Parallel Sequencing (MPS) of deafness genes. Given the importance of Lgn and its pathway partners in establishing planar cell polarity at the apical surface of the hair cell and its relevance to human deafness, we examined the phenotype and consequences of a similar Lgn mutation in mice. We report that $Lgn^{\Delta C}$ mice, harboring a targeted deletion in the coding regions of exons 13–15 (Konno et al. 2008), are profoundly deaf. We examined the changes that occur in the hair bundle during development, the effect of the mutation on gene and protein expression, and how the Lgn pathway interacts with the PCP pathway and the kinocilium. Given the viability of these mice, the results suggest that the Lgn GoLoco motifs are essential for the development of planar cell polarity in hair cells but dispensable in spindle orientation during cell division.

Materials and methods

Human subjects

The study was approved by the Human Subjects Committee of Bethlehem University. Members of Family α33 were ascertained with informed consent, as part of a larger study to identify genes involved in deafness in the Palestinian Arab deaf population (Brownstein et al. 2014). A medical history was collected regarding the deaf proband and other affected

individuals, including type and degree of hearing loss, age at onset, evolution and symmetry of the hearing impairment, use of hearing aids, the presence of tinnitus, medication, noise exposure, pathologic changes in the ear, and other relevant clinical manifestations, including vision problems, motor development, intellectual disability, and family history and consanguinity. Blood was drawn and genomic DNA was extracted for further analysis.

Targeted genomic enrichment and massively parallel sequencing

Three μg of genomic DNA from α33-1, the deaf proband, was sheared into 250–300 bp fragments. Library preparation, massively parallel sequencing, and bioinformatic analysis were performed as previously described (Brownstein et al. 2011, 2014). Sanger sequencing was performed on a 3130 Genetic Analyzer (Applied Biosystems).

Mice

The *Lgn*$^{\Delta C}$ targeted deletion line, *Lgn*$^{\Delta C/\Delta C}$, was previously described (Konno et al. 2008) and maintained on a C57BL/ 6 background. *LPT*/*LE* (*Vangl2*^{Lp}) mice were obtained from the Jackson Laboratory and maintained on a 129 × C57BL/6 mixed background. Ift88 mice were received from Prof. Bradley Yoder (University of Alabama). *Ift88*-$^{flox/flox}$ mice on a 129 × C57BL/6 mixed genetic background were bred and maintained on a 129 background. Pax2-Cre mice on a CD1 background were bred and maintained on a 129 background. *Ift88*$^{flox/flox}$ females were mated with Pax2-Cre males to obtain Pax2-Cre; *Ift88*$^{flox/flox}$ P0 newborns. Genotyping was performed using the KAPA Mouse Genotyping Kit (KAPA Biosystems). All animal procedures were approved by the Animal Care and Use Committee at Tel Aviv University (M-12-047), Emory University IACUC approved protocol #2001963, or the RIKEN Kobe Animal Experiments Committee according to the ‘guidelines for animal experiments at the RIKEN Center for Developmental Biology’ (AH14-04-33) and adhered to guidelines set forth by the National Institutes of Health Guide for the Care and Use of Laboratory Animals.

Hearing testing

Recording of auditory brainstem response (ABR) was used to assess hearing. P17 mice were anesthetized with an i.p. injection of Avertin (0.015 ml/g) and placed in an acoustic chamber (MAC-1, Industrial Acoustic Company), as previously described (Horn et al. 2013).

Magnetic resonance imaging

MRI scanning was performed on a 7T MRI scanner (Bruker). Five-month-old mice, anesthetized with 1–1.5 % isoflurane, were administrated with 4 ml/0.5 M MnCl2 (Sigma) in each nostril. Serial T2-weighted images were acquired with Multi-Slice Multi Echo fast spin echo sequence with the following parameters: 20 coronal slices, thickness 0.6 mm, FOV 2 × 2 cm, matrix dimensions of 256 × 128 pixels, TR/TE = 3300/50 ms, rare factor of 8 and 4 averages.

Scanning electron microscopy

Inner ears were dissected in cold PBS buffer and fixed in glutaraldehyde (2.5 % v/v in PBS) overnight at 4 °C. The organ of Corti was exposed, and the sample was treated with

alternating incubations in osmium tetroxide and thiocarbohydrazide (OTOTO method; Hunter-Duvar, 1978). Treated samples were critical point dried and gold-coated at the Faculty of Life Sciences Electron Microscopy Unit at Tel Aviv University and imaged with a JSM 540A scanning electron microscope (Jeol).

Immunolocalization

Mice were sacrificed according to ethical guidelines and inner ears were dissected out in cold PBS and fixed in paraformaldehyde (4 % v/v in PBS) for 2 h at room temperature or overnight at 4 °C. For GPSM2 antibody (Proteintech), ears were fixed with trichloroacetic acid (TCA) for 1 h on ice. Sensory epithelia were exposed and incubated in normal goat serum with Triton-X for 2 h at room temperature or overnight at 4 °C. Samples were incubated with the following primary antibodies in the indicated dilutions: C-terminal Lgn 1:500 (self-manufactured), N-terminal GPSM2 1:500 (Proteintech, 11608-2-AP), GNAI3 1:200 (Abcam, ab14246), Vangl2 1:200 (gift from Prof. Matthew Kelley, NIDCD, NIH), Fz3 1:500 (gift from Prof. Jeremy Nathans, Johns Hopkins University), aPKCζ 1:400(Santa Cruz, sc-216), acetylated α-tubulin 1:200 (Sigma Aldrich, T6793), NuMA 1:200 (Abcam, ab109262). Samples were incubated with secondary antibodies, and F-actin filaments were visualized with phalloidin, both conjugated to a variety of Alexa Fluorophores (Life Technologies). Nuclei were visualized with DRAQ5 (Life Technologies). In TCA-fixed samples, stereocilia were visualized using fluorescent-labeled peanut agglutinin (PNA, Life Technologies). Stained samples were mounted on Histobond microscope slides (Marienfeld GmbH) using a fluorescent mounting medium (GBI). Image acquisition was done with a Leica TCS SP5 II (Leica Microsystems). All images were taken from the basal area of the cochlea (lower 33 %) unless stated otherwise.

Quantification of hair bundle phenotypes

Adobe Photoshop was used to measure hair bundle orientation by drawing a line through the center of the hair bundle perpendicular to the line connecting the two edges of the hair bundle (modified from Jones et al. 2007). The angle between this line and the row of pillar cells was considered the orientation of a particular hair bundle. In wild-type mice, the degree of orientation is close to 0° and a 180° measurement indicates a completely inverted hair bundle. Positive and negative values indicate the direction in which the hair bundle deviated from the mediolateral axis. Hair bundles exhibiting split bundles were excluded from orientation analysis. Student's *t* test was used to determine significance.

qRT-PCR

RNA from plasma was isolated with TRIzol® reagent (Life Technologies). One μg of RNA was reversed transcribed. mRNA expression was evaluated with the TaqMan® Gene Expression Assay (Applied Biosystems) using the FastStart Universal Probe Master (Roche). Relative expression of the mRNAs was normalized to RLPO. Real-time PCR was performed in triplicate, including no-template controls. Samples were obtained from two homozygotes, four heterozygotes, and four unrelated controls.

Cochlear RNA was isolated from two half-ears of the same animal using the RNeasy kit (QIAGEN). 100 ng of RNA was reversed transcribed. mRNA expression was evaluated

using the TaqMan® Gene Expression Assay (Applied Biosystems) using the FastStart Universal Probe Master (Roche). Real-time PCR was done in triplicate, including no-template controls. Relative expression of the mRNAs was calculated with Tbp as the endogenous control to normalize the data and with Ptx3 to show that other mRNAs and their expression were not affected by the Lgn mutation (not shown, p value >0.2; $n = 3$). The experiment was repeated four times.

RNA from transfected cells was isolated using a standard phenol/chloroform nucleic acid extraction protocol. One μg of RNA per sample was reverse transcribed to cDNA. Reactions were prepared with PerfeCTa SYBR Green FastMix (Quanta Bioscience) using custom primers. Primer specificity and efficiency levels were verified by plotting calibration curves and performing a melting curve experiment on the same platform. The results were normalized to Gapdh expression using the ΔΔCt method (Livak and Schmittgen 2001). Three biological repeats ($n = 3$) were performed.

For all experiments, cDNA synthesis was performed using the High Capacity cDNA Reverse Transcription Kit (Applied Biosystems). mRNA expression was evaluated using the StepOnePlus™ Real-Time PCR System (Applied Biosystems). Data are presented as mean ± SEM, and statistical significance was determined using the one-tailed Student's t test.

Cell culture and Western blot

pEGFP(N1)-LGNwt-T2A-EGFP and pEGFP(N1)-LGNC-T2A-EGFP, with the latter carrying the *Lgn*$^{\Delta C}$ coding region, were created using the standard Gibson assembly protocol. The wild-type and ΔC sequences were subcloned from the pCAGGSS-containing vectors using the following Gibson assembly specialized primers The T2A linker polypeptide was subcloned from pLV hUbC-dCas9-T2A-GFP vector (Addgene plasmid # 531912). The pEGFP-N1 backbone vector was linearized using *Hind*III and *Bam*HI dual digest. Cloned plasmids were transformed into Stbl3 bacteria and verified by sequencing.

HEK293T cells were maintained with Dulbecco's modified Eagle's medium (DMEM) supplemented with 10 % FBS and 1 % penicillin/streptomycin. Cells were transfected with Lipofectamine 2000 (Invitrogen) with 2 μg of pDNA in 6 well plates. Cells were grown for 48-h post-transfection before harvesting cells.

Cells were lysed using RIPA buffer supplemented with cOmplete™, Mini, EDTA-free protease inhibitor cocktail (Roche). Protein concentration was measured using Protein Assay reagent (Bio-Rad) and the model 680 microplate reader (Bio-Rad). Samples were mixed with 3X sample buffer and boiled for 10 min. Fifty μg of protein was loaded onto a SDS polyacrylamide gel (SDS-PAGE) and transferred to a polvinylidenedifluoride (PVDF) membrane (Millipore) using a dry transfer apparatus (Bio-Rad). Membranes were blocked with 5 % milk blocking buffer and incubated overnight with an anti-GPSM2 antibody 1:1000 (Abcam, ab84571). ABX1/HP1 beta (Abcam, ab10478) was used as a loading control. Membranes were then incubated with a horseradish peroxidase 1:10,000 (HRP; Jackson Immuno Research) followed by SuperSignal West Pico Chemiluminescent Substrate (Thermo Scientific). Blot signals were detected using SuperRX film (FujiFilm) in a Kodak X-OMAT 2000 Processor or using a Fusion Fx (VilberLourmat),

Bioinformatics

Sequence alignment between human and mouse GPSM2/ Lgn proteins was produced with the BioEdit sequence alignment editor (Hall 1999). The image was rendered with Jalview 2.8.2 (Waterhouse et al. 2009). The boundaries of the TPR and GoLoco motifs were adapted from UniprotKB (The UniProt Consortium 2014) (accession numbers: P81274 and Q8VDU0 for human and mouse LGN accordingly). Structural alignment of the human (PBD code: 3SF4) (Yuzawa et al. 2011) and mouse (PDB code 4G2 V) (Pan et al. 2013) GPSM2/Lgn N-terminus TPR region was calculated and presented with the UCSF Chimera modeling system (Pettersen et al. 2004).

Results

A novel truncating variant in GPSM2 causes hearing loss

Family α33 is a consanguineous Palestinian family with congenital-to-prelingual severe-to-profound sensorineural hearing loss in two generations (Fig. 1a, b). One patient, III-2, was reported to have intellectual and physical disabilities; an MRI was unavailable to determine whether there were brain anomalies similar to CMCS. The pattern of hearing loss suggests an autosomal recessive mode of inheritance. Following screening for *GJB2* and other common deafness genes in the Palestinian population (Shahin et al. 2010), DNA from individual III-7 underwent TGE on a panel of 284 hearing loss-associated genes and subsequent MPS (Brownstein et al. 2014). Indel and copy number variants (CNV) were excluded, and the only homozygous candidate recovered in the single nucleotide variant (SNV) analysis was c.977G >A in the *GPSM2* gene (NM_013296.4) at chr1:109445771. The variant was validated by Sanger sequencing in all family members (example shown in Fig. 1c) and segregated with hearing loss in the family.

The variant is predicted to lead to a premature stop p.(Trp326*) in the eighth TPR motif. This nonsense variant was not detected in the NHLBI ESP Exome Variant Server (EVS; evs.gs.washington.edu/EVS/) or ExACBrowser (exac.broadinstitute.org/). The variant was not found in 100 ethnicity-matched hearing controls (200 chromosomes) or in 263 deaf Palestinian individuals (526 chromosomes). Quantitative RT-PCR (qRT-PCR) of mRNA derived from lymphoblasts of family members demonstrated that a stable but reduced transcript is expressed in p.Trp326* homozygotes (Fig. 1d), consistent with nonsense-mediated decay (NMD) (Kuzmiak and Maquat 2006).

Mice homozygous for the *Lgn*$^{\Delta C}$ allele are profoundly deaf

The p.Trp326* variant is the eighth *GPSM2* pathogenic variant reported in humans, all of which are truncating variants (Fig. 2a) (Walsh et al. 2010; Yariz et al. 2012; Doherty et al. 2012; Diaz-Horta et al. 2012; Almomani et al. 2013). To study the effect of truncating mutations in GPSM2 analogous to the human variants, we utilized a mouse model containing a deletion of the C-terminal GoLoco motifs, named *Lgn*$^{\Delta C}$ previously studied to examine the role of Lgn in the developing neuroepithelium (Konno et al. 2008). Hereafter, we will refer to the mouse gene and protein as Lgn. Human and mouse Lgn have a sequence identity and similarity of 91 and 94 % over the entire protein sequence, respectively (Fig. 2b). The TPR repeats also show a high degree of structural homology (Fig. 2c). There are no

structural data available for the region of the human GoLoco motifs. For these reasons, and due to the similarities between mouse and human inner ear structure and function, this mouse mutant is a relevant model to study the mechanisms of Lgn-induced deafness in humans. These mice have a targeted deletion removing the coding regions of the last three exons, but leaving the 3′-UTR of exon 15 intact. Previously described mice bearing mutations in Lgn either removed exon 5 (Tarchini et al. 2013) or removed exons 5–7 and were conditional for inner ear expression using Foxg1-Cre (Ezan et al. 2013); both are predicted to truncate the protein after the third TPR motif (Fig. 2a). The hearing status of these mutants was not addressed.

Unlike wild-type and heterozygous littermates, $Lgn^{\Delta C/\Delta C}$ mice do not exhibit a Preyer's reflex, a startle response to auditory stimulus, suggesting profound hearing loss. These mice do not circle or exhibit behavior associated with vestibular defects; therefore, the vestibule was not examined further. To conclusively test whether truncation of Lgn leads to hearing loss, P17 mice were tested for an auditory brainstem response (ABR) (Fig. 2d). $Lgn^{\Delta C/\Delta C}$ mice ($n = 4$) showed an increased hearing threshold across all tested frequencies relative to wild-type and heterozygous littermates ($n = 7$); an ABR response was not detected at the highest tested intensity (100 dB). The hearing phenotype in mice therefore mimics the profound congenital hearing loss observed in Family α33 and other human patients with CMCS (Walsh et al. 2010; Yariz et al. 2012; Doherty et al. 2012; Diaz-Horta et al. 2012; Almomani et al. 2013). In contrast to some CMCS patients, 5-month-old $Lgn^{\Delta C/\Delta C}$ mice did not show any overt differences compared to littermate controls in analysis of gross brain morphology by magnetic resonance imaging (MRI; Supplementary Fig. S1).

Hair bundle morphology is defective in mutant mice and deteriorates with age

To examine the effect of the Lgn truncation on the gross morphology of the hair bundles, we imaged the organ of Corti by scanning electron microscopy (SEM). Morphologically, stereocilia of inner hair cells (IHCs) of $Lgn^{\Delta C/\Delta C}$ mice appear short and stubby at P0, showing multiple rows of projections of uniform thickness instead of a single row of thick, long projections and shorter transient microvilli (Fig. 3a–d). These extra rows of stereocilia persist into adulthood, and become short and stubby by P15 (Fig. 3e–h), lacking both a flexible tapered base and a staircase structure, suggesting that such a hair bundle would not be able to deflect in response to sound. In outer hair cells (OHCs), hair bundles were much flatter than the V-shaped stereocilia of littermate controls (Fig. 3i–l). The degree of stereocilia flattening varied between hair cells, with 8.5 % of hair bundles appearing markedly flat (Fig. 3n; $n = 258$) as opposed to none at all in controls; some cells showing a ruffled hair bundle (Fig. 3n, o) and other cells presenting a normal V-shaped hair bundle. Some of the ruffled hair bundles appeared split, but with both hair bundle fragments still in contact and the stereocilia at the interface between the two bundles shorter and thinner than those of the bundles (Fig. 3p, q, arrowheads). This suggests that the hair bundle phenotypes may lie along a gradient and represent progressive effects of the Lgn mutation on hair bundle development, with the former phenotype representing an intermediate. A proportion of cells, 1.5–6.5 %, displayed a split hair bundle in which two separate stereocilia clusters formed at the apical surface of a single cell, with the kinocilium adjacent to only one such cluster (Fig. 3q, r), a phenotype never observed in control animals.

Developmentally, the phenotype severity increases over time. A severe phenotype in which two separate hair bundles were found relatively lateral and medial to each other in a single hair cell, rather than side by side, was evident only in the basal turns of P5 mutant cochlea (Fig. 3s–u). This phenotype was not found in more apical regions of P5 cochleae or at all in P0. This type of hair bundle phenotype was also found in P30 mice (Supplementary Fig. S2). At P0, split hair bundles were observed in the basal-most portion of the cochlea, decreasing in frequency apically and entirely absent from the middle turn of mutant mice (Fig. 3v, w), consistent with the base-to-apex developmental gradient along which the cochlea matures (Montcouquiol and Kelley 2003). At P5, a low frequency of split hair bundles appeared in the middle turn (Fig. 3x, y). These findings suggest that hair bundle splitting is a result of defective postnatal development and may be a consequence of hair bundle degeneration.

Hair bundles in mutant mice are misoriented

Hair bundles of mice with mutations in core PCP proteins maintain a V-shape but are severely misoriented (Montcouquiol et al. 2003; Curtin et al. 2003). Hair bundle orientation was quantified in $Lgn^{\Delta C/\Delta C}$ mice (Fig. 4). Our results show a broader distribution of hair bundle orientation in the second and third rows of outer hair cells, OHC2 (n = 235) and OHC3 (n = 260), and a slight effect in the first row of OHC, OHC1 (n = 242). No change was seen in IHCs (n = 222). An average of 11 % of hair cells was misoriented, but the degree of misorientation was mostly small. Overall, a minor but consistent misorientation of the hair bundle was observed, matching observations from a previously described Lgn mutant mouse (Ezan et al. 2013).

Increased expression of $Lgn^{\Delta C}$

In order to test the consequences of the $Lgn^{\Delta C}$ mutation, we tested the changes in mRNA and protein levels in the cochlea. Upon examination of cochlear extracts, we found that protein expression of full-length Lgn is reduced in heterozygotes and nearly absent in $Lgn^{\Delta C/\Delta C}$ mutant mice (Fig. 5a). Surprisingly, *Lgn* mRNA showed an increase in abundance, up to 3.5-fold, in $Lgn^{\Delta C/\Delta C}$ mice as compared to wild-type littermates (Fig. 5b). To test if this effect resulted from increased stability of the $Lgn^{\Delta C}$ mRNA, full-length and $Lgn^{\Delta C}$ alleles were cloned in-frame and upstream of a 2A-GFP (Fig. 5c) (Chan et al. 2011). Transfection into HEK 293 cells and measurement by qPCR demonstrated that $Lgn^{\Delta C}$ shows similar mRNA abundance to full-length *Lgn*, suggesting that the truncated ORF does not increase mRNA stability (Fig. 5d). Protein extracted from cells transfected with the $Lgn^{\Delta C}$ construct shows strong expression of a ~35 kD protein not present in any of the other samples (Fig. 5e). As the *Lgn* gene produces a single known transcript, these results suggest a truncated protein can be expressed potentially at even higher levels than wild type, raising the possibility that Lgn may regulate its own expression.

C-terminal domain of Lgn is essential for apical complexes in hair cells

Lgn forms a crescent pattern lateral to the hair bundle at the apical surface of hair cells in P0 cochleae, as does its binding partner Gαi (Fig. 6a–d). Gαi3 is a member of the inhibitory subclass of G proteins known to physically interact with Lgn (Mochizuki et al. 1996; Kaushik et al. 2003; Du and Macara 2004). Gαi proteins are anchored to the plasma membrane through a myristoylated residue and recruit Lgn to the cell cortex in MDCK cells

(Du and Macara 2004). We find that in mutant mice lacking the Gαi-binding GoLoco motifs in Lgn, in as much as $Lgn^{\Delta C}$ is translated in vivo, the apical localization of Lgn is lost (Fig. 6e–h), suggesting that Gαi binding is essential for the apical localization of Lgn. In order to further illuminate the interaction between Lgn and its known pathway proteins, we examined the localization of Gαi3 and aPKC in the inner ear of mutant mice. The Gαi3 compartment is maintained in mutants; however, Gαi3 also accumulates at the base of the stereocilia and colocalizes with the stereocilia filaments (Fig. 6i–l). aPKC, a member of the same apical complex as the *Drosophila* Lgn homolog Pins, is also polarized in the hair cell apical membrane, forming a medial crescent opposite Lgn and Gαi3 (Fig. 6m, n). In *Lgn* mutants, aPKC shows much weaker localization to the medial side of the apical surface and is enriched at the stereocilia (Fig. 6o, p). NuMA, another canonical Lgn binding partner important in mitotic spindle orientation, is sequestered in the nucleus of WT P0 mice, as in interphase cells in which it does not bind Lgn, and therefore is not expected to play a role in hair bundle polarity (Fig. 6q–t).

Kinocilium ablation affects Lgn compartmentalization

The kinocilium is required for proper formation of the hair bundle and PCP (Jones et al. 2007; Sipe and Lu 2011). Lgn has been shown to affect kinocilium positioning in the inner ear (Tarchini et al. 2013) and we asked whether the kinocilium might have an effect on Lgn. We examined the effect of kinocilium ablation on Lgn localization by examining the organ of Corti of *Ift88*-CKO mice created by Cre-loxP recombination, with mice harboring floxed *Ift88* but lacking Cre recombinase serving as controls (Jones et al. 2007) (Fig. 7a–f). In many cells, the Lgn compartment maintained its lateral polarization but extended more medially to the point of losing its crescent shape (Fig. 7d, arrows), changing the ratio of lateral to medial apical membrane. Concurrently, the hair bundle appears lower in the apical cortex compared to controls (Fig. 7e, arrows). In cases where the Lgn compartment formed an irregular shape, the hair bundle also developed irregularly (Fig. 7d, e, arrowheads).

The basal body, the organelle that anchors the kinocilium to the cell surface, is located within a region of the apical membrane known as the cytoplasmic channel, also called the fonticulus, an area that lacks actin fibers and allows the basal body to connect to the apical membrane (Lepelletier et al. 2013). Our results show that Lgn and Gαi3 are also absent from this region (Fig. 7a–l). The basal body and cytoplasmic channel are normally located at the center of the Lgn crescent at the hair bundle vertex; however, in the absence of the kinocilium, the basal body and cytoplasmic channel lose their ability to localize to the center of the Lgn/Gαi3 crescent (Fig. 7a–l).

Gαi3 presented a similar localization pattern as Lgn in the absence of a kinocilium (Fig. 7j–l). A single cell was found in a $Ift88^{CKO/CKO}$ cochlea bearing a kinocilium, likely the result of imperfect Cre expression (Fig. 7j–l, arrow).The hair bundle of this cell shows a properly formed Gαi3 compartment as well as a V-shaped hair bundle, suggesting that kinocilium delineation of apical compartments is a cell-autonomous process, independent of neighboring cells.

Immunostaining in *Ift88*-CKO mice showed a complementary phenotype in which the aPKC compartment became smaller in response to the change in the position of the hair bundle and

in accordance with the increase in Lgn/ Gαi distribution (Fig. 7m–r). Together, these results suggest the kinocilium has a role in the formation of the apical polarity complexes, including the basal body and the Lgn/ Gαi complex, in a cell-autonomous manner.

PCP proteins are upstream of the Lgn pathway and control the localization of apical protein compartments

Core PCP proteins dictate hair bundle orientation (Jones and Chen 2007) These proteins are enriched asymmetrically along hair cell membranes in wild-type mice, and their expression is diminished and their asymmetry is lost in PCP mutant mice (Montcouquiol et al. 2006). To examine whether Lgn affects PCP protein localization, we performed immunostaining of Vangl2 and Fz3 in ears from P0 $Lgn^{\Delta C/\Delta C}$ mice (Fig. 8a–h). Vangl2 and Fz3 were similarly partitioned in both control and mutant samples, suggesting that Lgn is not involved in PCP protein localization, as previously found (Ezan et al. 2013; Tarchini et al. 2013).

We also examined the localization of Lgn and Gαi3 in Looptail mice carrying a mutation in Vangl2 (Kibar et al. 2001), where stereocilia are severely misoriented but maintain the characteristic V-shape (Montcouquiol et al. 2003). Interestingly, Lgn and Gαi3 formed the same crescent-shaped compartments formed in mutant mice, albeit rotated along with the hair bundle (Fig. 8i–p). This result suggests the core PCP pathway is upstream to the orientation of the Lgn complex, consistent with previously reported results on *Lgn* mutant mice (Tarchini et al. 2013). Therefore, a Vangl2 mutation does not affect the relative partitioning of the crescent and the central localization of the basal body within the Lgn crescent, indicating that this gene does not affect the formation of the Lgn complex and its associated structures while orienting the complex. In *Vangl2* mutants, only the orientation of apical complexes was defective; in contrast, *Ift88* mutants show defects both in partitioning and in the shape of the apical complexes. Complex partitioning and orientation are consistent in these mutants with the shape of the mature hair bundles.

These data suggest that core PCP proteins direct the orientation of the Lgn/Gai/aPKC complex and its associated apical structures, which form a separate polarity module that governs intrinsic cellular polarity.

Discussion

New deafness genes and novel pathogenic variants in these genes are being identified at an increasing rate due to the technological advances in DNA sequencing (Brownstein et al. 2012). Many of the deafness genes discovered in this process have no known role in inner ear biology, highlighting the importance of mouse models to illuminate their role in the development and maintenance of the auditory system. In this work, we report a new human pathogenic variant in *GPSM2*, demonstrate the utility of the $Lgn^{\Delta C}$ mouse as a model for human GPSM2-based hearing loss, characterize the inner ear defects associated with this mutation, and identify proteins and organelles that interact with Lgn during hair bundle morphogenesis.

Distinct functional domains of Lgn for survival and apical polarity

The p.Trp326* variant is the eighth pathogenic nonsense variant reported in humans (Fig. 1), all of which are also nonsense variants. A similar case, in which pathogenic variants in a gene are almost exclusively nonsense variants, has been reported in the *ARID1B* gene; over 60 pathogenic nonsense variants in this gene, and only a single missense variant have been reported, explaining 70 % of the cases of Coffin-Siris syndrome (Sim et al. 2015). Transcripts of *GPSM2* alleles carrying nonsense variants have been identified using Sanger sequencing (Walsh et al. 2010; Yariz et al. 2012), although mRNA abundance was not examined. Truncating variants often trigger NMD and reduce gene expression to 5–25 % of wild-type expression, as reported here, and we predict that nonsense variants likely cause NMD for all reported human variants.

Despite the lower abundance of *GPSM2*/*LGN* mRNA in the lymphoblasts of adolescent and adult humans, targeted knockdown of Lgn in the skin of embryonic mice demonstrates that 80 % reduction in Lgn expression results in dehydration and death due to compromised barrier function (Williams et al. 2011). Transfection of such knockdown mice with $Lgn^{\Delta C}$–*mRFP* rescued the lethal phenotype by partially restoring spindle orientation function in the skin. This essential role of Lgn in murine skin development suggests that at least partial Lgn activity is required for survival (Williams et al. 2011).

Experimental truncation of Pins, the *Drosophila* homolog of Lgn, demonstrated that a truncated protein lacking the GoLoco domain was able to orient the mitotic spindle in cultured *Drosophila* S2 cells as efficiently as full-length Pins (Johnston et al. 2009), suggesting that the GoLoco motifs are not required for spindle orientation and rather might only play a regulatory role (Du and Macara 2004). In contrast, loss of the GoLoco motifs precludes Lgn apical localization, suggesting an essential role for this motif in the mammalian inner ear. Previous reports demonstrate that Gαi is a suitable candidate to translate PCP cues to effector activity (Ezan et al. 2013; Tarchini et al. 2013), strengthened by Gαi3 presence in the kinocilium as primary cilia are known for their role in signaling (Goetz and Anderson 2010). We speculate that based on kinocilium localization, Gαi may serve a dual role, both as a physical bridge between Lgn and the membrane and as part of a signaling pathway in the kinocilium affecting apical protein localization.

Similar to the effect on Gαi, aPKC is also enriched in the stereocilia of $Lgn^{\Delta C}$ mutant mice. This is in contrast to Lgn^{BF} homozygote mice in which the aPKC domain extends laterally (Tarchini et al. 2013). This is consistent with the finding that in cochlear explants, ectopically expressed Ed::Lgn, which localizes uniformly at the apical surface of hair cells, sequesters aPKC to the center of the apical membrane (Tarchini et al. 2013). In $Lgn^{\Delta C/\Delta C}$ mice, lateral extension of the aPKC domain is a minor phenomenon. One might speculate that a truncated Lgn peptide may be localizing both aPKC and Gαi to the stereocilia in $Lgn^{\Delta C/\Delta C}$ mice; however, the total loss of Lgn apical localization suggests this is not the case.

NuMA, short for Nuclear Mitotic Apparatus and functionally homologous to the *Drosophila* Mud protein, is found in a complex with Lgn and Gαi in virtually all examined tissues in which these proteins have a role in spindle orientation. NuMA is sequestered to the nucleus

in interphase cells and is released into the cytosol upon breakdown of the nuclear envelope. This cytosolic influx of NuMA is believed to release Lgn from its closed conformation and increases its affinity for Gαi in mammals. As hair cells are post-mitotic prior to the development of planar cell polarity and thus do not form spindle poles at this stage, this might explain why NuMA does not appear to be involved in this process.

Independent roles of core PCP proteins and the Lgn apical complex

While hair bundle positioning is severely misoriented in PCP mutants, hair bundle intrinsic polarity is unaffected, resulting in the classic V- or W-shaped stereocilia (Montcouquiol et al. 2003; Curtin et al. 2003). This implies that a separate pathway is responsible for executing the polarity cues dictated by PCP proteins, and that aberrant PCP signaling might merely misorient the proteins in this second pathway. Additionally, asymmetric localization of PCP proteins is crucial for their function (Montcouquiol et al. 2006). Our results demonstrate that Vangl2 and Fz3, canonical PCP proteins, localize asymmetrically independent of Lgn, but Lgn/Gαi localization is dependent on Vangl2. These findings validate the previously described dependence of Lgn and Gαi on PCP proteins, and the independence of PCP protein asymmetry upon Lgn (Ezan et al. 2013; Tarchini et al. 2013). PCP and apical surface proteins, such as Lgn, Gαi and aPKC, have been suggested to be two independent polarity systems; we find it useful to describe these pathways as a separate but displaying a one-way dependence of Lgn complex genes on the core PCP pathway.

The kinocilium is required to delineate the apical compartments that determine hair bundle contour

Several mouse models carrying mutations in genes with similar effects on stereocilia contour have been described recently (Grimsley-Myers et al. 2009; Sipe et al. 2013; Ezan et al. 2013; Tarchini et al. 2013; Gegg et al. 2014; Kirjavainen et al. 2015), suggesting these genes are all involved in generating the hair bundle's intrinsic polarity. The encoded proteins are involved in basal body/kinocilium positioning or function, critical processes in hair bundle morphogenesis (Schwander et al. 2010). Most importantly, the interface between the mInsc/Lgn/Gαi and the Par3/Par6/aPKC complexes outlines the exact contour of the stereocilia, and interference with this interface affects the contour of the resulting hair bundle (Tarchini et al. 2013).

Here, we show that the kinocilium itself also plays a role in delineating the interface between these apical compartments. Our results demonstrate that loss of the kinocilium creates an extended Lgn/Gαi domain at the expense of aPKC and the resulting hair bundle forms at this new interface, and that the position of the basal body is altered from the center of the Lgn/Gαi crescent. Mutants lacking functional Mkks, a protein essential for kinocilium function, show a similar extended Gαi3 domain to Ift88 mutants with a non-centralized cilium within the bounds of the Gαi3 domain (Ezan et al. 2013). These results suggest that a functional kinocilium is required for compartment delineation and strengthen the finding that crosstalk occurs between the kinocilium and the lateral apical cortex (Ezan et al. 2013).

We hypothesize that the kinocilium regulates Lgn distribution in accordance with the intrinsic orientation dictated by PCP signaling, and Lgn regulates the distribution of the

aPKC complex. It has been suggested that the kinocilium migrates in two motions, one from the cell center to the lateral junction and the second back toward the cell center (Tarchini et al. 2013). As the Lgn compartment forms and localizes during this second inward motion, it is plausible that this is when this interaction takes place.

The Lgn$^{\Delta C}$ mouse as a model for GPSM2-based hearing loss in humans

GPSM2 was first identified as the causative gene for DFNB82 hearing loss in a Palestinian family (Walsh et al. 2010), followed by the discovery of additional pathogenic variants in other ethnic groups (Yariz et al. 2012; Almomani et al. 2013). Hearing loss in these patients ranges from severe to profound. *GPSM2* was also identified as the causative gene in CMCS (Doherty et al. 2012), a syndromic form of hearing loss presenting with several brain malformations but rarely exhibiting neurodevelopmental abnormalities other than deafness. Subsequently, most of the patients diagnosed with isolated deafness were found to harbor the brain anomalies characteristic of CMCS, suggesting that *GPSM2* pathogenic variants only lead to a syndromic, and not a non-syndromic, form of deafness. Only one deaf family member of Family α33, found to harbor a truncating variant in *GPSM2*, was reported to have intellectual and physical disabilities. While there is often variability in the symptoms of CMCS patients, even between siblings, the disabilities in this patient were much more severe than the phenotype in other documented CMCS patients; there, it is unlikely to be due to the *GPSM2* variant.

We show that *Lgn*$^{\Delta C}$ mice present with similar audiological findings to the human patients. Deafness in humans carrying homozygous *GPSM2* variants is either congenital or prelingual. Hearing onset in mice occurs around P15, and mutant mice were tested and found to be profoundly deaf at P17, suggesting the condition is congenital in the model as well. This conclusion is supported by phenotypic data showing morphological defects detrimental to hearing during development.

Genotype–phenotype correlation

The *Lgn*$^{\Delta C}$ allele lacks its three terminal exons, while the *Lgn*^{BF} allele has an exon 5 deletion, leading to a frameshift and premature stop codon similar in length to the human p.Arg127* variant. As crystal structures suggest that the TPR repeat domain has its own inherent structural stability, it is reasonable to predict that deletion of TPR 7–8 would abolish mInsc binding. This suggests that if these truncated alleles are expressed, *Lgn*$^{BF/BF}$ mice produce shorter Lgn proteins than *Lgn*$^{\Delta C/\Delta C}$ mice. Accordingly, *Lgn*$^{\Delta C/\Delta C}$ hair bundles show a less severe phenotype than *Lgn*$^{BF/BF}$ hair bundles; hair bundles termed “type III” (Tarchini et al. 2013; see Fig. 3c) were not observed at all in *Lgn*$^{\Delta C/\Delta C}$ at P0 and microtubules do not appear significantly perturbed in the latter. Furthermore, the frequency of split hair bundles in *Lgn*$^{BF/BF}$ cochleae (termed “type II”) ranges from 15 to 50 % with an average of roughly 30 %, while *Lgn*$^{\Delta C/\Delta C}$ has a much lower frequency of split hair bundles. As both engineered alleles are expressed on a C57BL6 background, this suggests that the most severe phenotype of *Lgn*^{BF} mice results from a more severe truncation of the *Lgn* gene (Fig. 2a).

The genotype–phenotype correlation found in the mouse contrasts with reports in humans, in which no correlation was found and phenotypic variation was seen in patients within the same family (Doherty et al. 2012); indeed, the most severe variant reported to date, p.Arg127*, showed a weak brain phenotype and was initially considered to cause non-syndromic deafness (Walsh et al. 2010). This suggests genetic background may play a role in the manifestation of pathogenic variants.

Model of Lgn function and hair bundle development

The staircase structure of individual hair cells and the uniform orientation of stereocilia across the organ of Corti are essential to converting mechanical vibrations to an electrochemical signal. Loss of robust orientation and aberrant hair bundle shape are sufficient to cause profound hearing loss; however, the effect of the $Lgn^{\Delta C}$ mutation on the shape of stereocilia differs between IHCs and OHCs. IHC microvilli develop into a uniform field of short stereocilia, whereas OHC stereocilia flatten and split into separate hair bundles. Truncation of Lgn has been shown to cause more dispersed basal body positioning and it has been suggested that the role of the Insc/Lgn/Gαi complex in the inner ear is to maintain the basal body/kinocilium at the vertex of the forming bundle (Tarchini et al. 2013). As it has been shown that the basal body migrates by confined Brownian motion during development and suggested that this constraint is imposed by cytoskeletal elements (Lepelletier et al. 2013), the Lgn complex may be a good candidate for this function.

The process of actin hair bundle maturation appears to be independent of the kinocilium. Hair cells lacking kinociliary links, in which the kinocilium is not adjacent to the hair bundle (Webb et al. 2011), and hair bundles that lack a kinocilium altogether (Jones et al. 2007; Sipe and Lu 2011) all nonetheless demonstrated the emergence and maturation of actin-based stereocilia. This suggests that the kinocilium guides the proper morphogenesis of stereociliary hair bundles but is not required for the maturation of microvilli into stereocilia. Given that hair bundles of wild-type IHCs and OHCs differ in their mature shapes, it is reasonable to presume that actin dynamics during hair bundle morphogenesis respond differently to insults to kinocilium movement. We therefore hypothesize that these related yet distinct developmental programs are the cause for the different phenotypes seen in IHCs and OHCs.

We propose that the hair bundle phenotypes observed in $Lgn^{\Delta C/\Delta C}$ OHCs lie along a gradient, beginning with flattening of the hair bundle, subsequent ruffling, and finally splitting (Fig. 3m–r). The exacerbated phenotype of P5 and P30 hair cells compared to P0 hair cells suggests that the splitting occurs late in the abnormal development of mutant hair bundles. Hair bundles that appear on the verge of splitting have shorter, thinner filaments at the interface between two hair bundles (Fig. 3p, q), and in other cells, the two half bundles have no filaments in contact (Fig. 3r). In these latter cells, the filaments in the part of the bundle that is not in contact with the kinocilium cluster together. As a result, the hair cells are unable to provide the signals required for mechanotransduction, leading to profound hearing loss in both mouse models for GPSM2 human deafness and in human patients with GPSM2 truncating variants.

At the molecular level, *Lgn*$^{\Delta C}$ undergoes translation in vitro. In terms of mRNA, *Lgn*$^{\Delta C}$ does not seem to be more stable than the WT allele in vitro, suggesting that transcriptional upregulation is a more plausible explanation of the greater abundance of *Lgn*$^{\Delta C}$ mRNA in the cochleae of homozygote mice. The difference between these findings may stem from the loss of endogenous regulatory elements. This hypothetical autoregulation mechanism would mean either that Lgn$^{\Delta C}$ is a gain-of-function that increases its own transcription directly or indirectly, or the endogenous Lgn downregulates its own expression, and the *Lgn*$^{\Delta C}$ mutant represents a loss-of-function.

Based on these molecular findings, the varying phenotypes in different Lgn mouse models and the lethality of Lgn-depletion in murine skin (Williams et al. 2011), we hypothesize that truncating variants in Gpsm2/Lgn in both humans and mice are not inactivating but rather result in the formation of a truncated protein product with reduced activity. Partial activity of a truncated protein is sufficient to perform most of its roles in development, although loss of regulation by Gαi may be the cause in part of the brain malformations and hearing loss associated with CMCS.

Supplementary Material

Refer to Web version on PubMed Central for supplementary material.

Acknowledgments

This work was supported by the Human Frontier Science Program RGP0012/2012 (K. B. A., P. C., F. M., D. S.); National Institutes of Health (NIDCD) R01DC011835 (K. B. A., M. K.); I-CORE Program of the Planning and Budgeting Committee and The Israel Science Foundation, Centers of Excellence in Gene Regulation in Complex Human Disease, Grant No. 41/11 (K. B. A.) and in Integrated Structural Cell Biology, Grant No. 1775/12 (E. T, M. L.); and a TEVA Pharmaceutical Industries Ltd. as part of the Israeli National Network of Excellence in Neuroscience (NNE) (Y. B.). This work was performed in partial fulfillment of the requirements for a Ph.D. degree by Yoni Bhonker at the Sackler Faculty of Medicine, Tel Aviv University, Israel. We wish to thank Megy Cemel and Michal Meir for their valuable contributions.

References

Almomani R, Sun Y, et al. GPSM2 and Chudley-McCullough syndrome: a Dutch founder variant brought to North America. Am J Med Genet Part A. 2013; 161A(5):973–976. [PubMed: 23494849]

Bhonker, Y., Ushakov, K., et al. Human gene discovery for understanding development of the inner ear and hearing loss. In: Romand, R., Varela-Neito, I., editors. Development of auditory and vestibular systems. Academic Press; New York: 2014. p. 107-128.

Brownstein Z, Friedman LM, et al. Targeted genomic capture and massively parallel sequencing to identify genes for hereditary hearing loss in Middle Eastern families. Genome Biol. 2011; 12(9):R89. [PubMed: 21917145]

Brownstein Z, Bhonker Y, et al. High-throughput sequencing to decipher the genetic heterogeneity of deafness. Genome Biol. 2012; 13(5):245. [PubMed: 22647651]

Brownstein Z, Abu-Rayyan A, et al. Novel myosin mutations for hereditary hearing loss revealed by targeted genomic capture and massively parallel sequencing. Eur J Hum Genet. 2014; 22(6):768–775. [PubMed: 24105371]

Chan HY, Sivakamasundari V, et al. Comparison of IRES and F2A-based locus-specific multicistronic expression in stable mouse lines. PLoS ONE. 2011; 6(12):e28885. [PubMed: 22216134]

Curtin JA, Quint E, et al. Mutation of *Celsr1* disrupts planar polarity of inner ear hair cells and causes severe neural tube defects in the mouse. Curr Biol. 2003; 13(13):1129–1133. [PubMed: 12842012]

Diaz-Horta O, Sirmaci A, et al. *GPSM2* mutations in Chudley-McCullough syndrome. Am J Med Genet A. 2012; 158A(11):2972–2973. [PubMed: 22987632]

Doherty D, Chudley AE, et al. *GPSM2* mutations cause the brain malformations and hearing loss in Chudley-McCullough syndrome. Am J Hum Genet. 2012; 90(6):1088–1093. [PubMed: 22578326]

Du Q, Macara IG. Mammalian Pins is a conformational switch that links NuMA to heterotrimeric G proteins. Cell. 2004; 119(4):503–516. [PubMed: 15537540]

Ezan J, Lasvaux L, et al. Primary cilium migration depends on G-protein signalling control of subapical cytoskeleton. Nat Cell Biol. 2013; 15(9):1107–1115. [PubMed: 23934215]

Gegg M, Böttcher A, et al. Flattop regulates basal body docking and positioning in mono- and multiciliated cells. eLife. 2014; 3:e03842.

Gilissen C, Hoischen A, et al. Disease gene identification strategies for exome sequencing. Eur J Hum Genet. 2012; 20(5):490–497. [PubMed: 22258526]

Goetz SC, Anderson KV. The primary cilium: a signalling centre during vertebrate development. Nat Rev Genet. 2010; 11(5):331–344. [PubMed: 20395968]

Grimsley-Myers CM, Sipe CW, et al. The small GTPase Rac1 regulates auditory hair cell morphogenesis. J Neurosci. 2009; 29(50):15859–15869. [PubMed: 20016102]

Hall T. BioEdit: a user-friendly biological sequence alignment editor and analysis program for Windows 95/98/NT. Nucleic Acids Symp Ser. 1999; 41(1999):95–98.

Horn HF, Brownstein Z, et al. The LINC complex is essential for hearing. J Clin Invest. 2013; 123(2): 740–750. [PubMed: 23348741]

Hunter-Duvar IM. A technique for preparation of cochlear specimens for assessment with the scanning electron microscope. Acta Oto-Laryngol Suppl. 1978; 351:3–23.

Jacobo A, Hudspeth AJ. Reaction–diffusion model of hair-bundle morphogenesis. Proc Natl Acad Sci USA. 2014; 111(43):15444–15449. [PubMed: 25313064]

Johnston CA, Hirono K, Prehoda KE, Doe CQ. Identification of an Aurora-A/PinsLINKER/Dlg spindle orientation pathway using induced cell polarity in S2 cells. Cell. 2009; 138(6):1150–1163. [PubMed: 19766567]

Jones C, Chen P. Planar cell polarity signaling in vertebrates. BioEssays. 2007; 29(2):120–132. [PubMed: 17226800]

Jones C, Roper VC, et al. Ciliary proteins link basal body polarization to planar cell polarity regulation. Nat Genet. 2007; 40(1):69–77. [PubMed: 18066062]

Kaushik R, Yu F, et al. Subcellular localization of LGN during mitosis: evidence for its cortical localization in mitotic cell culture systems and its requirement for normal cell cycle progression. Mol Biol Cell. 2003; 14(8):3144–3155. [PubMed: 12925752]

Kibar Z, Vogan KJ, et al. *Ltap*, a mammalian homolog of *Drosophila Strabismus/Van Gogh*, is altered in the mouse neural tube mutant Loop-tail. Nat Genet. 2001; 28(3):251–255. [PubMed: 11431695]

Kirjavainen A, Laos M, et al. The Rho GTPase Cdc42 regulates hair cell planar polarity and cellular patterning in the developing cochlea. Biol Open. 2015; 4(4):516–526. [PubMed: 25770185]

Konno D, Shioi G, et al. Neuroepithelial progenitors undergo LGN-dependent planar divisions to maintain self-renewability during mammalian neurogenesis. Nat Cell Biol. 2008; 10(1):93–101. [PubMed: 18084280]

Kuzmiak HA, Maquat LE. Applying nonsense-mediated mRNA decay research to the clinic: progress and challenges. Trends Mol Med. 2006; 12(7):306–316. [PubMed: 16782405]

Lepelletier L, de Monvel JB, et al. Auditory hair cell centrioles undergo confined brownian motion throughout the developmental migration of the kinocilium. Biophys J. 2013; 105(1):48–58. [PubMed: 23823223]

Livak KJ, Schmittgen TD. Analysis of relative gene expression data using real-time quantitative PCR and the 2(−Delta Delta C(T)) method. Methods. 2001; 25(4):402–408. [PubMed: 11846609]

Mapelli M, Gonzalez C. On the inscrutable role of Inscuteable: structural basis and functional implications for the competitive binding of NuMA and Inscuteable to LGN. Open Biol. 2012; 2(8):120102. [PubMed: 22977735]

Mauser JF, Prehoda KE. Inscuteable regulates the Pins-Mud spindle orientation pathway. PLoS One. 2012; 7(1):e29611. [PubMed: 22253744]

Mochizuki N, Cho G, et al. Identification and cDNA cloning of a novel human mosaic protein, LGN, based on interaction with G alpha i2. Gene. 1996; 181(1):39–43. [PubMed: 8973305]

Montcouquiol M, Kelley MW. Planar and vertical signals control cellular differentiation and patterning in the mammalian cochlea. J Neurosci. 2003; 23(28):9469–9478. [PubMed: 14561877]

Montcouquiol M, Rachel RA, et al. Identification of *Vangl2* and *Scrb1* as planar polarity genes in mammals. Nature. 2003; 423(6936):173–177. [PubMed: 12724779]

Montcouquiol M, Sans N, et al. Asymmetric localization of Vangl2 and Fz3 indicate novel mechanisms for planar cell polarity in mammals. J Neurosci. 2006; 26(19):5265–5275. [PubMed: 16687519]

Pan Z, Shang Y, et al. Structural and biochemical characterization of the interaction between LGN and Frmpd1. J Mol Biol. 2013; 425(6):1039–1049. [PubMed: 23318951]

Pettersen EF, Goddard TD, et al. UCSF Chimera—a visualization system for exploratory research and analysis. J Comput Chem. 2004; 25(13):1605–1612. [PubMed: 15264254]

Richardson GP, de Monvel JB, et al. How the genetics of deafness illuminates auditory physiology. Ann Rev Physiol. 2011; 73:311–334. [PubMed: 21073336]

Schaefer M, Shevchenko A, et al. A protein complex containing Inscuteable and the Gα-binding protein Pins orients asymmetric cell divisions in Drosophila. Curr Biol. 2000; 10(7):353–362. [PubMed: 10753746]

Schwander M, Kachar B, et al. The cell biology of hearing. J Cell Biol. 2010; 190(1):9–20. [PubMed: 20624897]

Shahin H, Walsh T, et al. Five novel loci for inherited hearing loss mapped by SNP-based homozygosity profiles in Palestinian families. Eur J Hum Genet. 2010; 18(4):407–413. [PubMed: 19888295]

Shearer AE, Smith RJH. Massively Parallel Sequencing for genetic diagnosis of hearing loss: the new standard of care. Otolaryngol Head Neck Surg. 2015; 153(2):175–182. [PubMed: 26084827]

Sim JCH, White SM, et al. ARID1B-mediated disorders: mutations and possible mechanisms. Intractable Rare Dis Res. 2015; 4(1):17–23. [PubMed: 25674384]

Sipe CW, Lu X. Kif3a regulates planar polarization of auditory hair cells through both ciliary and non-ciliary mechanisms. Dev Camb Engl. 2011; 138(16):3441–3449.

Sipe CW, Liu L, et al. Lis1 mediates planar polarity of auditory hair cells through regulation of microtubule organization. Development. 2013; 140(8):1785–1795. [PubMed: 23533177]

Stevermann L, Liakopoulos D. Molecular mechanisms in spindle positioning: structures and new concepts. Curr Opin Cell Biol. 2012; 24(6):816–824. [PubMed: 23142476]

Tall GG, Gilman AG. Resistance to inhibitors of cholinesterase 8A catalyzes release of Gαi-GTP and nuclear mitotic apparatus protein (NuMA) from NuMA/LGN/Gαi-GDP complexes. Proc Natl Acad Sci USA. 2005; 102(46):16584–16589. [PubMed: 16275912]

Tarchini B, Jolicoeur C, Cayouette M. A molecular blueprint at the apical surface establishes planar asymmetry in cochlear hair cells. Dev Cell. 2013; 27(1):88–102. [PubMed: 24135232]

The UniProt Consortium. UniProt: a hub for protein information. Nucleic Acids Res. 2014; 43:D204–D212. [PubMed: 25348405]

Walsh T, Shahin H, et al. Whole exome sequencing and homozygosity mapping identify mutation in the cell polarity protein GPSM2 as the cause of nonsyndromic hearing loss DFNB82. Am J Hum Genet. 2010; 87(1):90–94. [PubMed: 20602914]

Wang J, Mark S, et al. Regulation of polarized extension and planar cell polarity in the cochlea by the vertebrate PCP pathway. Nat Genet. 2005; 37(9):980–985. [PubMed: 16116426]

Waterhouse AM, Procter JB, et al. Jalview Version 2—a multiple sequence alignment editor and analysis workbench. Bioinformatics. 2009; 25(9):1189–1191. [PubMed: 19151095]

Webb SW, Grillet N, et al. Regulation of PCDH15 function in mechanosensory hair cells by alternative splicing of the cytoplasmic domain. Development. 2011; 138(8):1607–1617. [PubMed: 21427143]

Williams SE, Beronja S, et al. Asymmetric cell divisions promote Notch-dependent epidermal differentiation. Nature. 2011; 470(7334):353–358. [PubMed: 21331036]

Yariz KO, Walsh T, et al. A truncating mutation in *GPSM2* is associated with recessive non-syndromic hearing loss. Clin Genet. 2012; 81(3):289–293. [PubMed: 21348867]

Yuzawa S, Kamakura S, et al. Structural basis for interaction between the conserved cell polarity proteins Inscuteable and Leu-Gly-Asn repeat-enriched protein (LGN). Proc Natl Acad Sci USA. 2011; 108(48):19210–19215. [PubMed: 22074847]

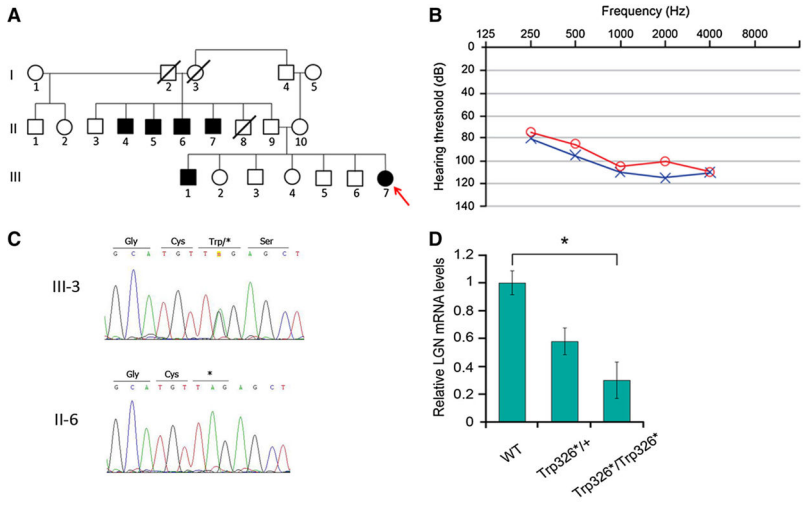

Fig. 1.

A novel truncating variant in GPSM2/LGN. **a** Pedigree for Family α33. *Circles* indicate females, *square* indicate males. *Black shapes* indicate individuals affected by hearing loss. DNA from individual III-7 (*arrow*) underwent targeted capture and high-throughput sequencing. **b** Audiogram for individual III-7 showing profound hearing loss across all tested frequencies. *Red*, *right* ear; *blue*, *left* ear. **c** Sanger sequencing of the G-to-A transition occurring in a heterozygote carrier (III-3) and homozygote (II-6) for the p.Trp326* variant. **d** qPCR of *GPSM2*/*LGN* using allele non-specific primers on cDNA derived from human lymphoblasts. **p* value = 0.01, ***p* value <0.05. *Error bars* represent standard error of mean (Color figure online)

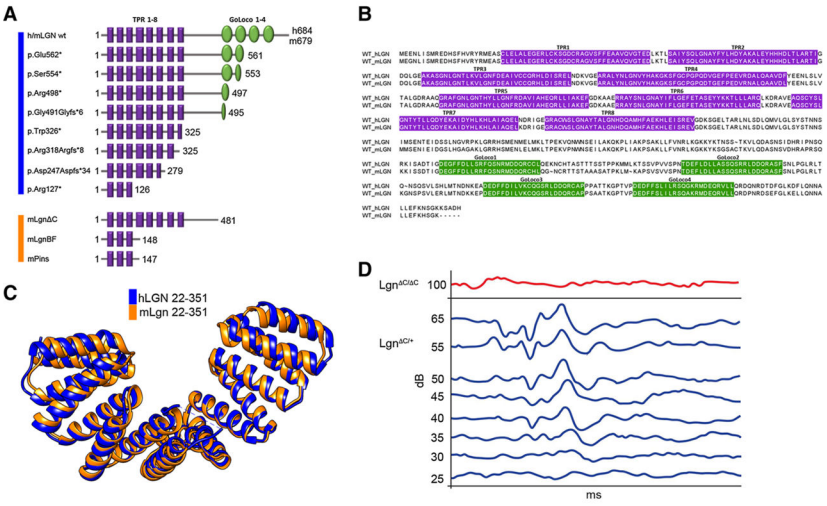

Fig. 2.

Human *GPSM2LGN* pathogenic variants and phenotypes are represented in *Lgn* mouse mutants. **a** Schematic diagram of all known mutant GPSM2/LGN human (Walsh et al. 2010; Yariz et al. 2012; Doherty et al. 2012; Diaz-Horta et al. 2012; Almomani et al. 2013) and mouse alleles (Konno et al. 2008; Ezan et al. 2013; Tarchini et al. 2013), demonstrating the effect of nonsense or frameshift variants on the predicted protein. **b** Sequence alignment of the mouse and human GPSM2/LGN protein. TPR motifs are highlighted in *purple*, GoLoco motifs are highlighted in *green*. **c** Structural alignment of the human (*blue*, PBD code 3SF4) (Yuzawa et al. 2011) and mouse (*gold*, PDB code 4G2V) (Pan et al. 2013) GPSM2/LGN N-terminus TPR region, indicating high structural similarity with a root mean square distance (RMSD) of 1.104 Å. **d** Representative auditory brainstem response (ABR) test demonstrates a lack of response in $Lgn^{\Delta C/\Delta C}$ mice at the highest intensity tested, compared to normal responses in littermate controls. Seven littermate controls and 4 mutant mice were tested; no difference was seen between heterozygotes and wild-type mice. All frequency differences were significant (p <0.00001). *ms* milliseconds, *dB* decibels (Color figure online)

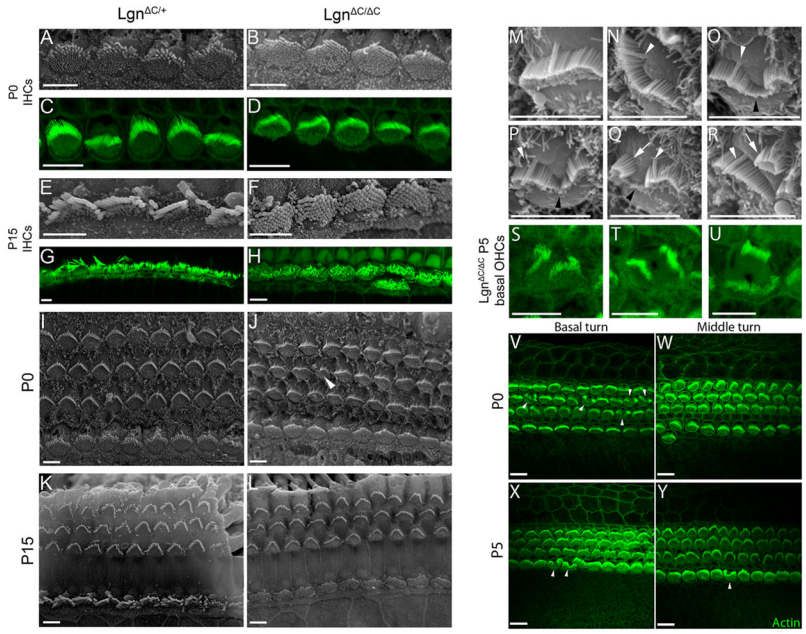

Fig. 3.

The Lgn truncation causes defective morphogenesis of hair bundles of inner and outer hair cells. **a–d** At P0, control IHCs have a few rows of thick, elongated stereocilia and medial microvilli; *Lgn*$^{\Delta C/\Delta C}$ IHCs have a field of stereocilia of seemingly uniform thickness extending all the way to the medial cell junction. **e–h** At P15, mutant mice show multiple thick elongated rows of stereocilia compared to wild-type mice. **i–l** *Three rows* of outer hair cells and one *row* of inner hair cells are arranged in the cochlea derived from wild-type mice. Outer hair cells of *Lgn*$^{\Delta C/\Delta C}$ mice have flatter hair bundles than littermate controls at P0 and display split bundles in some hair cells (*arrowhead*). **m–r** Severe bundle defects are observed in outer hair cells of mutants. *Arrows* indicate split bundles, *white arrowheads* indicate the kinocilium, and *black arrowheads* mark the degenerate stereocilia at the boundary of splitting bundles. **s–u** OHCs showing medially and laterally localized sub-bundles were found only in the basal region of P5 Lgn mutants. **v–y** Representative images of hair cell phenotypes in the basal and middle turns at P0 and P5, showing that split hair bundles appear in the developmentally younger middle turn only at P5. *Arrowheads* indicate split or nearly split hair bundles. Five tiled images were taken per region per genotype. *Scale bars* = 5 μm

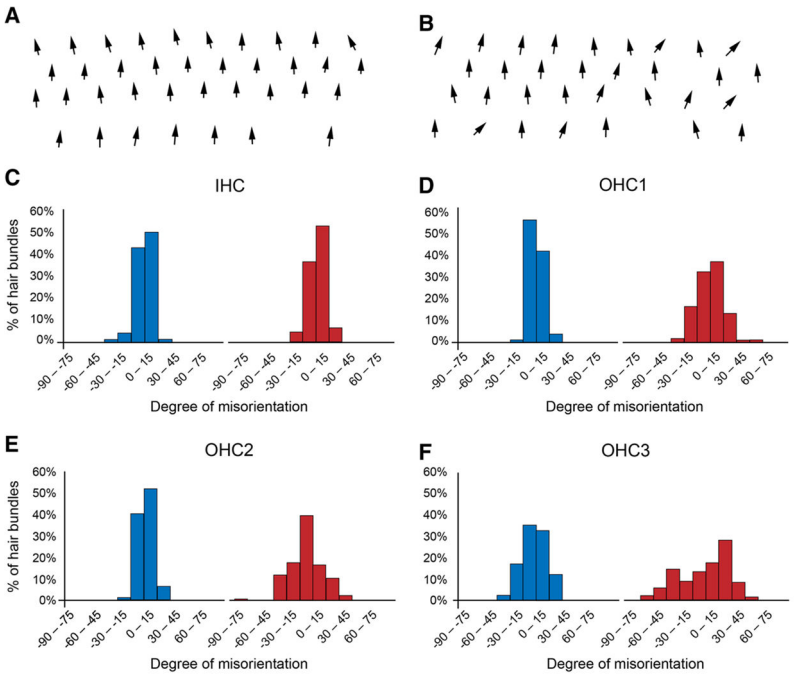

Fig. 4.

$Lgn^{\Delta C/\Delta C}$ mice have a broader distribution of hair bundle angles than control mice. **a, b** Schematic of hair bundle orientations in $Lgn^{\Delta C/+}$ controls and $Lgn^{\Delta C/\Delta C}$ mutants. Gaps indicate deformed or split hair bundles for which orientation cannot be determined. **c–f** Hair bundle distribution grouped by row (*IHC* inner hair cell; *OHC* outer hair cell; number increases along the mediolateral axis) in control (*blue*) and mutant (*red*) *Lgn* P0 mice ($n \geq$ 99 per mouse; ≥3 mice per genotype). IHCs appear to be unaffected overall in mutant mice (Color figure online)

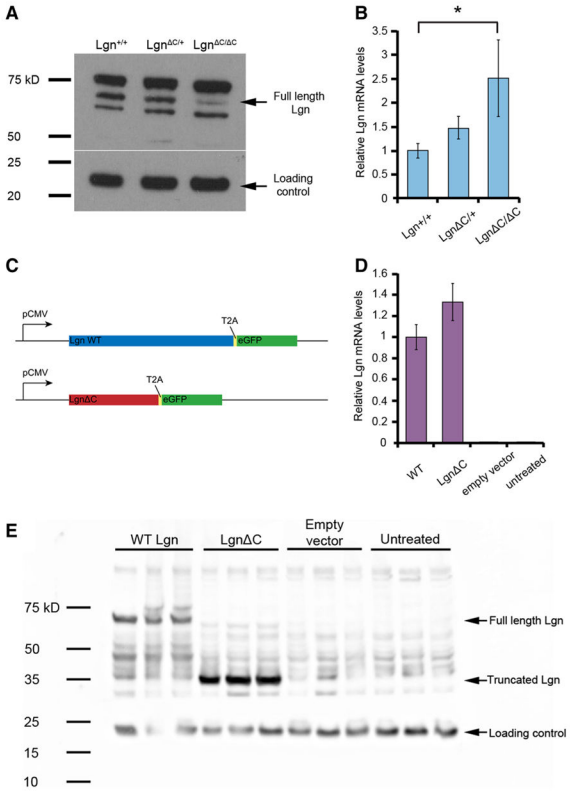

Fig. 5.

Lgn is expressed in vitro. **a** Western blot using a C-terminal antibody demonstrates a decrease in *a* <75 kD band in heterozygote samples and significant reduction of this band in $Lgn^{\Delta C/\Delta C}$ mutant samples of protein extracts from the inner ears of P0 mice. HP1 was used as a loading control. **b** *Lgn* mRNA abundance as detected by qPCR using primers specific to both full-length and ΔC alleles. Levels represent the average of three biological repeats. The difference between wild-type and mutant samples was significant at *p* value <0.05. Ptx3 was used as an endogenous control and its expression was not affected by the *Lgn* mutation. **c** Schematic diagram of Lgn expression vectors. 2A peptides are self-cleaving, resulting in Lgn proteins that are not fused to eGFP. **d** Expression levels of Lgn constructs in HEK293 cells showing no significant difference between the two Lgn alleles (*p* value >0.09). Lack of detectable signal in the empty vector and untreated controls demonstrates the specificity of the primers to mouse Lgn only. *Error bars* represent standard error of mean. **e** Western blot using an anti-N-terminal antibody capable of recognizing both full-length and truncated Lgn. Ectopic $Lgn^{\Delta C}$ is detected at higher levels than ectopic WT Lgn. HP1 was used as a loading control

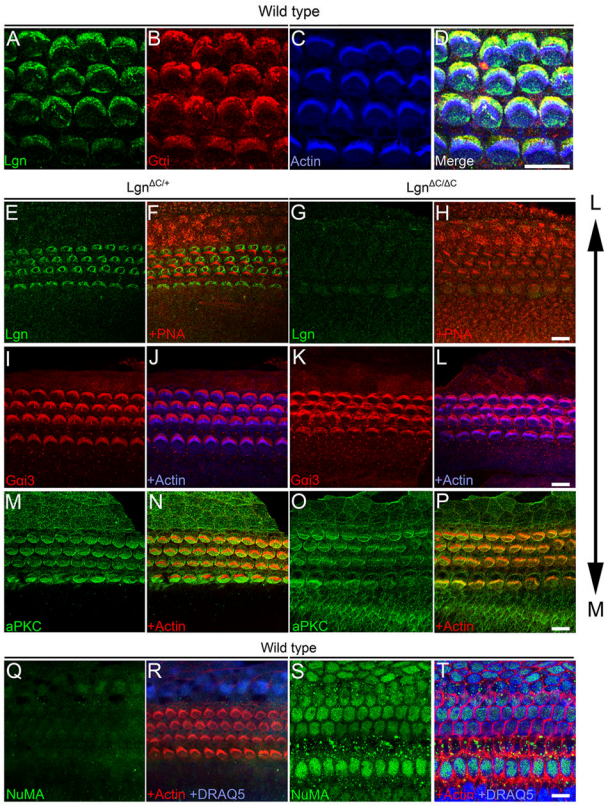

Fig. 6.

Lgn pathway proteins form apical compartments in the hair bundle of P0 mice. **a–d** Lgn (*green*) and Gαi3 (*red*) form colocalizing crescents lateral to the hair bundle (*blue*). Both proteins appear to colocalize to the kinocilium as well. **e–h** Lgn apical localization is lost in mutant mice. An antibody raised against the N-terminus of Lgn was used to allow detection of truncated peptides. **i–l** Gαi3 expression in Lgn mutant mice and control littermates. Gαi3 can be found colocalized with the hair bundle and accumulated at the base of the stereocilia in mutant mice. **m–p** aPKC forms a compartment medial to the hair bundle and is absent from lateral side of the hair bundle. In Lgn mutant mice, aPKC medial localization is weaker and protein localization is enriched in the stereocilia. **q–t** NuMA is mostly absent from the apical surface of hair cells (**q–r**), yet is highly enriched in the nucleus (**s–t**). The images are presented in a different focal plane, in order to focus on the hair bundle or nucleus. *Scale bar* = 10 μm, spatial axis: *L* lateral, *M* medial (Color figure online)

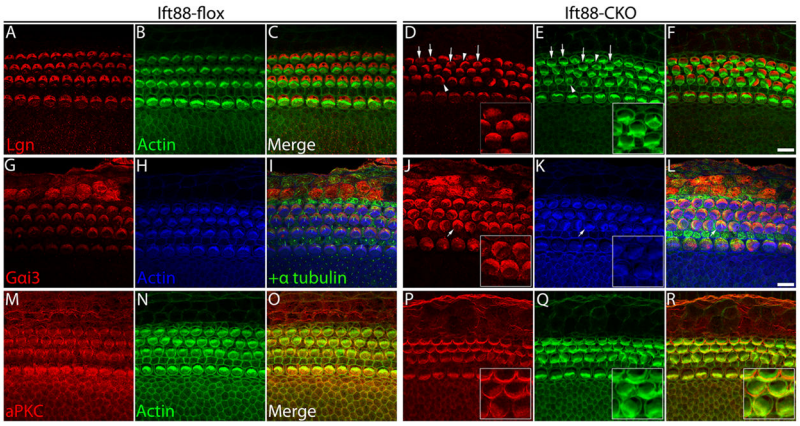

Fig. 7.

The kinocilium is required for proper delineation of Lgn pathway protein compartments in P0 mice. *Ift88*$^{flox/flox}$ mice have floxed Ift88 alleles but not Cre recombinase (**a–f**) Lgn crescents extend medially in the absence of the kinocilium. The cytoplasmic channel localizes to the tip of the hair bundle vertex and dissociates from this position in mutant mice. *Arrows* indicate flattened and lowered hair bundles, arrowheads indicate irregularly shaped hair bundles and Lgn crescents. (**g–l**). The Gαi crescent shows a similar expression pattern to Lgn in kinocilia-ablated cells. A single cell in which a kinocilium formed normally maintains proper bundle structure and orientation, microtubule network localization, and Gαi and cytoplasmic channel localization (**j–l**, *arrow*). **m–r** aPKC localization extends medially in *Ift88-CKO* mice. *Scale bar* = 10 μm

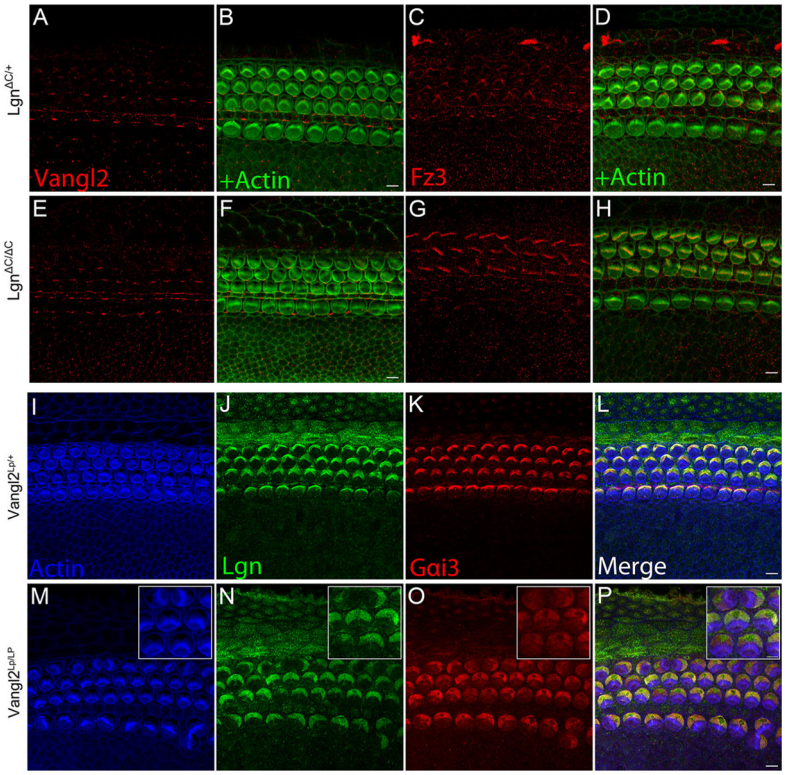

Fig. 8.

PCP proteins control Lgn pathway proteins. **a–h** Vangl2 and Fz3 are normally partitioned in *Lgn*$^{\Delta C/\Delta C}$ P0 mice. Hair bundle staining is an assay artifact resulting from use of unfiltered serum; and Fz3 is not known to stain the hair bundle. **i–p** Lgn and Gαi3 are misoriented in *Vangl2*$^{Lp/Lp}$ mice in the association with and to the same degree as the actin hair bundle. Unlike *Lgn*$^{\Delta C/\Delta C}$ mice, both the hair bundle and apical structures (Lgn/Gαi complex, cytoplasmic channel) undergo proper morphogenesis. *Scale bar* = 5 μm